Journal of Hazardous Materials 171 (2009) 491–499

Contents lists available at ScienceDirect

Journal of Hazardous Materials

journal homepage: www.elsevier.com/locate/jhazmat

# Effects of crystalline structures and surface functional groups on the adsorption of haloacetic acids by inorganic materials

Patiparn Punyapalakul[a,b,*], Suwat Soonglerdsongpha[b], Chutima Kanlayaprasit[a], Chawalit Ngamcharussrivichai[c,d], Sutha Khaodhiar[a]

[a] Department of Environmental Engineering, Faculty of Engineering, Chulalongkorn University, Bangkok 10330, Thailand
[b] National Research Center of Excellence for Environmental and Hazardous Waste Management (NCE-EHWM), Chulalongkorn University, Bangkok 10330, Thailand
[c] Department of Chemical Technology, Faculty of Science, Chulalongkorn University, Bangkok 10330, Thailand
[d] Center of Excellence for Petroleum, Petrochemicals and Advanced Materials, Chulalongkorn University, Bangkok 10330, Thailand

ARTICLE INFO

*Article history:*
Received 7 April 2009
Received in revised form 6 June 2009
Accepted 8 June 2009
Available online 16 June 2009

*Keywords:*
Haloacetic acids
Hexagonal mesoporous silicate
Zeolite
Adsorption

ABSTRACT

The effects of the crystalline structure and surface functional groups of porous inorganic materials on the adsorption of dichloroacetic acid (DCAA) were evaluated by using hexagonal mesoporous silicates (HMS), two surface functional group (3-aminopropyltriethoxy- and 3-mercaptopropyl-) modified HMSs, faujasite Y zeolite and activated alumina as adsorbents, and compared with powdered activated carbon (PAC). Selective adsorption of $HAA_5$ group was studied by comparing single and multiple-solute solution, including effect of common electrolytes in tap water. Adsorption capacities were significantly affected by the crystalline structure. Hydrogen bonding is suggested to be the most important attractive force. Decreasing the pH lower than the $pH_{zpc}$ increased the DCAA adsorption capacities of these adsorbents due to electrostatic interaction and hydrogen bonding caused by protonation of the hydronium ion. Adsorption capacities of $HAA_5$ on HMS did not relate to molecular structure of $HAA_5$. Common electrolytes did not affect the adsorption capacities and selectivity of HMS for HAA5, while they affected those of PAC.



## 1. Introduction

Haloacetic acids (HAAs) are common disinfection by-products (DBPs) usually found in chlorinated drinking water. Oxidative reactions involving free chlorine or bromine and natural organic matter (NOM) may form nine common species of HAAs. The types and amount of compounds formed depends mainly on the composition of water and on the dose of halogenic chemical oxidants. Several researchers have suggested an association between HAAs and the incidence of cancers, including bladder, rectal and colon cancer [1,2]. Moreover, some HAAs, like mono- and di-chloroacetic acid, are not only used as intermediates for the manufacture of drugs, dyes and chemicals, but also as herbicides [3,4]. The US Environmental Protection Agency [5] has regulated the total maximum contaminant level (MCL) in drinking water of five HAAs ($HAA_5$), monochloro-, dichloro-, trichloro-, monobromo- and dibromoacetic acid (MCAA, DCAA, TCAA, MBAA and DBAA), to be less than 60 μg/l. The USEPA classified DCAA as a probable human carcinogen (Group B2) and TCAA as a possible human carcinogen (Group C).

The control of HAAs is a challenge and a necessity because of the uncertainty of their generation mechanisms upon halogenation of natural organic matter (NOM) in drinking water, the high hydrophilicity, high yield at pH < 7 and the health effects that are putatively associated with them [6]. Tung et al. [7] found that in general GAC had a much lower adsorption capacity for HAAs (and especial trichloroacetic acid) than for THMs.

Xie and Zhou [8] reported that biological activated carbon (BAC) is more efficient for haloacetic acid (HAA) removal than autoclaved GAC, and this was attributed to the biodegradation of HAAs by microbes. However, the disadvantages of activated carbon are their wide pore size distribution, heterogeneous structure and a low selectivity for adsorption. Hexagonal mesoporous silicate (HMS) has been studied extensively in the adsorption and catalysis fields and has a mesoscale pore and silanol as a surface functional group. The HMS surface can be modified with various groups and methods to enhance the specific characteristics (e.g., organic ligand modification). Punyapalakul and Takizawa [9] studied DCAA adsorption on HMS and functionalized HMSs at a high concentration (ppm level) and found that the physical characteristic of synthesized HMSs did not affect the DCAA adsorption capacity, whilst a higher concentration of surface amino-functional groups on the HMS gave a higher positive charge leading to an enhanced adsorption capacity for DCAA. In addition, a combination of mercapto- and amino-

* Corresponding author. Tel.: +66 8 218 6686; fax: +66 2 218 6666.
*E-mail address:* patiparn.p@eng.chula.ac.th (P. Punyapalakul).

0304-3894/$ – see front matter © 2009 Elsevier B.V. All rights reserved.
doi:10.1016/j.jhazmat.2009.06.024

functional groups caused a higher surface complexity, produced more active surface sites, and gave a higher DCAA adsorption capacity than amino-functionalized HMS. At low concentration (ppb level), effects of hydronium ion and hydroxide ion on both electrostatic interaction and hydrogen bonding are supposed to be stronger that can make adsorption mechanisms different from high concentration level. Moreover, the molecular sieve of the micropore scale combined with the positive charge of faujasite Y zeolite (NaY and HY) caused by the positive counter ion on the crystalline structure, is suggested to enhance the adsorption capacity of negative charged HAAs. However, the effect of the crystalline structure combined with the surface functional groups of silicate material on the adsorption capacity at low concentrations (ppb) of HAAs is still unclear.

The objective of this study was to investigate the effect of surface and pore structure, and surface functional groups of synthesized adsorbents, as well as the effects of pH on the $HAA_5$ adsorption kinetic and isotherms. All of the experiments to investigate the adsorption efficiencies and mechanisms were conducted at a low concentration of DCAA (0–400 ppb), as a model HAA, consistent with USEPA standards. Batch adsorption experiments were carried out with three types of inorganic materials with different crystalline structure (HMS, zeolite and alumina), along with powdered activated carbon (Shirasagi S-10, Japan, EnvironChemicals Ltd.). In addition, two methods of organic-ligand grafting onto HMS, with amino- and mercapto-functional groups, was employed to investigate the effects of different physico-chemical characteristics on the adsorption capacities for DCAA. The obtained data were used to describe and to compare how the DCAA, as a model HAA, adsorption capacities were affected by the crystalline structures and surface functional groups. Moreover, selective adsorption of $HAA_5$ groups was studied by comparing single and multiple-solute solution, including effect of common electrolytes in tap water.

## 2. Materials and methods

### 2.1. HMS synthesis

HMS was prepared by the following method. 1.0 mol of tetraethoxysilane (TEOS) (Acros Oganics) was dissolved into a mixture of water (29.6 mol), dodecylamine (Acros Oganics) (0.27 mol) and ethanol (Carlo Erba) (9.09 mol) under magnetic stirring at 200 rpm. The reaction mixture was aged at ambient temperature for 18 h, then filtered and air-dried on a glass plate. The product was calcined in air under static conditions at 650 °C for 4 h to remove the organic template [10], with a temperature increase rate, up to 650 °C, of 1 °C/min to preserve the crystalline structure.

### 2.2. Synthesis of functionalized HMSs

Modification of HMS with surface functional groups was prepared by a standard pre-functional groups grafting procedure as follows: 1.0 mol of tetraethoxysilane (TEOS) was added to a mixture of water (50 mol), dodecylamine (0.25 mol) and ethanol (10.25 mol) under vigorous stirring. The stirring was continued for 30 min and then 0.25 mol of either 3-aminopropyltriethoxysilane (APTES) or 3-mercaptopropyltrimethoxysilane (MPTMS) was added to yield either A-HMS or M-HMS, respectively. The reaction mixtures were vigorously stirred (200 rpm) for 20 h at ambient temperature, and then filtered and air-dried at room temperature on a glass plate for 24 h. Residual organosilanes and surfactant were removed by Soxhlet extraction for 72 h with ethanol [11].

### 2.3. Activated alumina and NaY zeolite preparation

Activated alumina and NaY zeolite were activated by calcination in air using a muffle furnace. The temperature was elevated at a rate of 1 °C/min up to 400 °C and holding at this temperature for 3 h.

### 2.4. HY zeolite preparation

HY zeolite was prepared by exchanging the sodium ion of NaY zeolite with ammonium ion by adding 1 M ammonium nitrate at a ratio of liquid-to-solid of 20 (w/v). The mixture was stirred at 60 °C for 2 h, filtered and washed with milli-Q water (18.2 MΩ). This exchange procedure was repeated twice. The final retentate was dried at 100 °C for 12 h and calcined at 400 °C as described above.

### 2.5. Characterization of adsorbents

Powder X-ray diffraction (XRD) patterns of synthesized adsorbents were recorded on a powder diffractometer equipped with Cu Kα radiation (Bruker AXS Model D8 Discover). The BET specific surface area was calculated from the nitrogen adsorption isotherms, as measured at 77 K by a Micromeritic model: ASAP 2020 version 1.04H, at a relative pressure between 0.04 and 0.20. Pore diameter and mesopore volume were calculated by the D-H method. Surface functional groups were investigated after drying at 105 °C for 4 h by FT-IR spectrophotometer (Nicolet Impact 410). Surface charges of all adsorbents were determined by acid–base titration with HCl and NaOH as described by Punyapalakul and Takizawa [12].

### 2.6. Adsorption experiments

Evaluation of the adsorption kinetics was performed by varying the contact time from 0–72 h under batch conditions with a DCAA concentration of 100 μg/l and 2 g/l of adsorbent. The pH and ionic strength of the solution were fixed using 0.01 M phosphate buffer at pH 7. Samples were agitated in a shaking water bath at 150 rpm and 25 °C, and then filtered through a glass filter (GF/C, poresize 0.45 μm). The first 10 ml of filtrate was discarded and the rest was harvested for analysis following USEPA method 552.2 by gas chromatography using an electron capture detector (GC/ECD) Agilent GC6890. To analyze the adsorption rate of the synthesized adsorbents and PAC, the pseudo-first-order equation of Lagergren (1) and the pseudo-second-order rate (2) were evaluated based on the experimental data. The pseudo-first-order and pseudo-second-order kinetic models are expressed as follows:

$$\ln(q_e - q_t) = \ln q_e - k_1 t \quad (1)$$

$$\frac{t}{q_t} = \frac{1}{k_2 q_e^2} + \frac{t}{q_e} \quad (2)$$

where $k_1$ and $k_2$ are the Lagergren rate constant ($h^{-1}$) and pseudo-second-order rate constant ($g\,mg^{-1}\,h^{-1}$), and $q_e$ and $q_t$ are the amounts of DCAA sorbed at equilibrium and at time $t$ (h), respectively. The experimental data were plotted as $\ln(q_e - q_t)$ versus time for fitting the first-order rate or as $t/q_t$ versus time for the second-order rate.

The adsorption isotherm evaluation was performed by varying the DCAA concentration from 10 to 400 μg/l under batch conditions using 2 g/l adsorbent. The pH of solution was fixed by 0.01 M phosphate buffers at either pH 5, 7 or 9. Samples were then shaken, filtered and harvested for analysis following USEPA method 552.2 as described above. The experimental data was analyzed using the adsorption isotherm models of Langmuir (3) and Freundlich (4) as:

$$q_e = \frac{q_m K_L C_e}{1 + K_L C_e} \quad (3)$$

$$q_e = K_F C_e^{1/n} \quad (4)$$

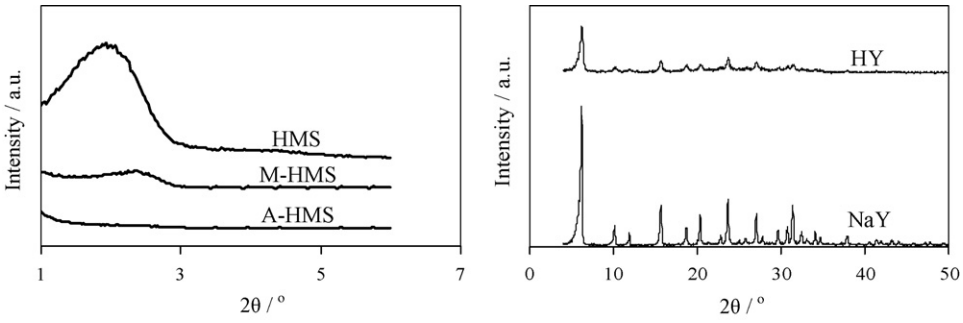


**Fig. 1.** Representative X-ray powder diffraction patterns of pristine HMS, A-HMS, M-HMS, NaY and HY.

where $K_L$ is the adsorption equilibrium constant, $q_m$ is the maximum adsorption capacity (μg/g), $C_e$ is the equilibrium concentration, $q_e$ is the adsorption capacity at equilibrium (μg/g), $K_F$ and $n$ are Freundlich constants.

## 3. Results and discussion

### 3.1. Physical characteristics of adsorbents

Fig. 1 shows representative X-ray powder diffraction patterns of synthesized HMSs and zeolites. According to the XRD pattern, synthesized pristine HMS (pure silica HMS) exhibited a strong single diffraction peak at $2\theta = 2.2^\circ$, and a weak peak around 4.3° due to the hexagonal porous structure, although the obtained structure of the prepared HMS was not likely to be a complete hexagonal porous structure since, compared with other hexagonal mesoporous silicates, it should show an XRD pattern consisting of (1 0 0), (1 1 0), (2 0 0) and (2 1 0) diffractions. However, the XRD patterns of M-HMS and A-HMS exhibited very board peak, indicated that their porous structures were lost by the pre-grafting method compared with pristine HMS. It might be caused by protonation of APTES under acid or neutral condition. Protonated aminopropyltriethoxysilane (APTES) can cross-link with the surface silanol groups of silicate species, and it might play a strong influence on the self-assembly of surfactant, leading to weaker interactions of the silicate species with the surfactant template [13]. The diffraction patterns of the microporous zeolites NaY and HY (Fig. 1) show spectra which are similar to those in the reference database [14], supporting the formation of zeolite frameworks. The sharp XRD peaks indicated that the zeolites have a high degree of crystallinity.

Nitrogen adsorption–desorption isotherms of HMS, the two functional group modified HMSs (A-HMS and M-HMS), zeolite (NaY and HY) and PAC are shown in Fig. 2. The surface area and pore size of all applied adsorbents were calculated from nitrogen adsorption–desorption isotherm data and are summarized in Table 1. PAC had the largest BET specific surface area, followed closely by M-HMS, and then pristine HMS and NaY zeolite, whilst HY zeolite, A-HMS and finally activated alumina had a much lower BET surface area. Moreover, the pore size of synthesized HMSs was apparently affected by the functional group grafting method (Table 1). The larger pore size (diameter) of A-HMS might be caused by disorder of the hexagonal structure of the silica base. The DCAA's molecular size, being 0.69 and 0.46 nm in width and length, respectively, means that the pore size did not affect the accessibility of DCAA into the mesopore of the adsorbents and PAC. However, the accessibility of DCAA to the internal surface of NaY and HY zeolite was suggested to be low compared to other porous adsorbents.

SEM micrographs of pristine HMS, A-HMS, M-HMS and PAC revealed that HMS and the two modified HMSs were in the form of aggregated spherical particles (Fig. 3), which is consistent with the report of Gontier and Tuel [15]. Moreover, the modification method affected the particle size with slightly larger A-HMS and M-HMS particles, yet the particle sizes of all HMSs are, however, still very small compared with PAC.

### 3.2. Zero point of charge

The surface charge density of synthesized adsorbents, activated alumina and PAC were measured by acid/base titration, and show distinct characteristics (Fig. 4). Pristine HMS had a zero point of charge ($pH_{ZPC}$) at a pH range between 4 and 6, whilst the $pH_{ZPC}$ of M-HMS, A-HMS, NaY, HY, activated alumina and PAC were 6.2, 9.5, 7.8, 4.5, 7.3 and 9.5, respectively, as shown in Table 1. Grafted organic moieties affected the surface charge of HMS, with 3-aminopropyltriethoxy-groups (A-HMS) increasing the surface charge of HMS significantly, yet 3-mercaptopropyl-groups (M-HMS) only changed the surface charge of HMS a relatively small amount. The silanol groups and organic functional groups on the surface of synthesized HMSs, NaY and HY zeolite can be ionized at different pH values as summarized by following equations [16]:

$$pH < pH_{ZPC}: \equiv Si\text{–}OH + H^+ \rightarrow \equiv Si\text{–}OH_2{}^+$$

$$pH > pH_{ZPC}: \equiv Si\text{–}OH + OH^- \rightarrow \equiv Si\text{–}O^-$$

$$pH < pH_{ZPC}: \equiv Si\text{–}R\text{–}NH_2 + H^+ \rightarrow \equiv Si\text{–}R\text{–}NH_3{}^+$$

**Table 1**
Physical characteristic of HMS, A-HMS, M-HMS, NaY zeolite, HY zeolite, PAC and activated alumina.

| Adsorbents | Pore diameter (nm) | BET surface area ($m^2$/g) | Pore volume ($mm^3$/g) | Particle size (μm) | Surface functional groups | $pH_{ZPC}$ |
|---|---|---|---|---|---|---|
| HMS | 2.60 | 712 | 773 | 0.46 | Silanol | 4.5–5.5 |
| A-HMS | 3.95 | 262 | 147 | 0.50 | Amino, silanol | 9.5 |
| M-HMS | 2.48 | 912 | 433 | 0.49 | Mercapto, silanol | 6.2 |
| NaY zeolite | 0.74 | 653 | 326 | 2–5 | $Na^+$ | 7.8 |
| HY zeolite | 0.74 | 370 | 201 | 2–5 | Brönsted acid | 4.5 |
| Activated alumina | – | 147 | – | 0.8 | Hydroxyl | 7.3 |
| PAC | 1.90 | 980 | 276 | ≈36 | Carboxyl, phenyl and others | 9.5 |

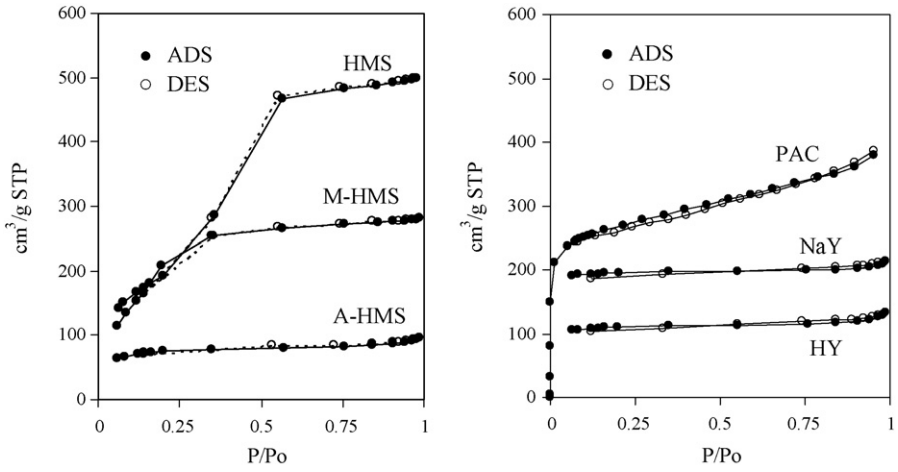


**Fig. 2.** $N_2$ adsorption–desorption isotherms of synthesized HMSs, PAC, NaY and HY.

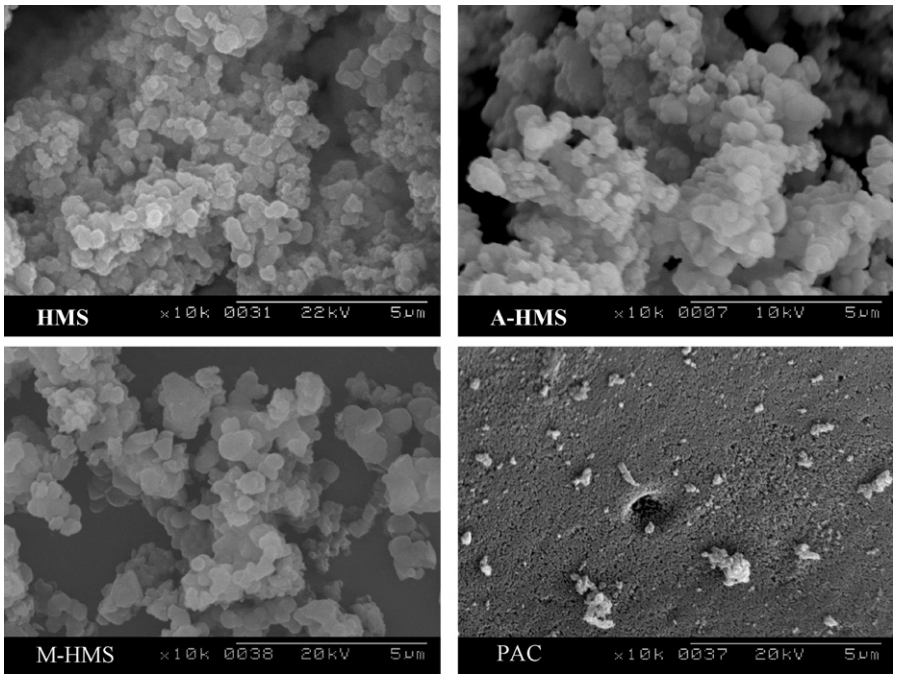


**Fig. 3.** Representative SEM pictures of pristine HMS, A-HMS, M-HMS and PAC at 10,000× magnifications.

$$pH > pH_{ZPC}: \equiv Si\text{–}R\text{–}NH_2 + OH^- \rightarrow \equiv Si\text{–}R\text{–}NH_2OH$$

$$pH < pH_{ZPC}: \equiv Si\text{–}R\text{–}SH + H^+ \rightarrow \equiv Si\text{–}R\text{–}SH_2{}^+$$

$$pH > pH_{ZPC}: \equiv Si\text{–}R\text{–}SH + OH^- \rightarrow \equiv Si\text{–}R\text{–}SHOH$$

### 3.3. Adsorption kinetic

The evaluation of the DCAA adsorption kinetics is summarized in Fig. 5, where the DCAA adsorption on PAC attained equilibrium faster than on the other adsorbents. DCAA concentration decreased dramatically in the first 10 min and reached equilibrium stage approximately at the sixth hour. For HMS, the two surface functionalized HMSs (A-HMS and M-HMS), activated alumina, NaY and HY zeolite, the amount of adsorbed DCAA increased significantly during the first and sixth hour and reached equilibrium stage approximately at the twentieth hour. In order to analyze

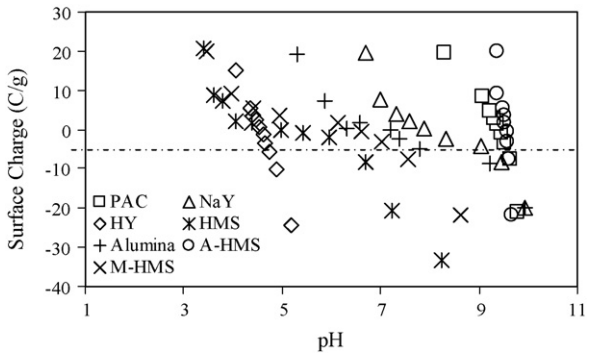


**Fig. 4.** Surface charges density of synthesized HMSs, PAC, activated alumina NaY and HY zeolite as a function of pH at ionic strength (IS) 0.01 M.

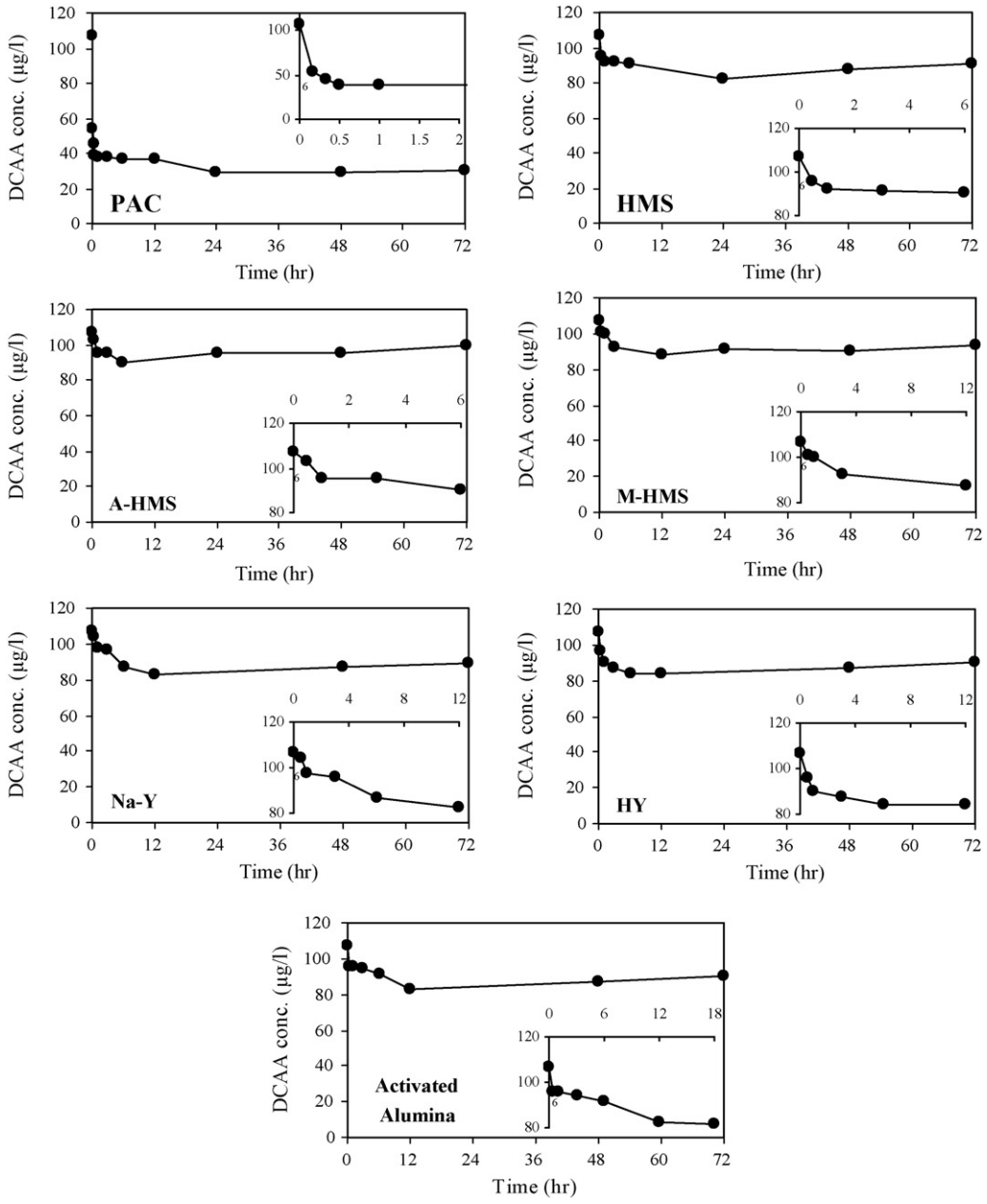


**Fig. 5.** DCAA adsorption kinetics of PAC, HMS, A-HMS, M-HMS, NaY, HY and activated alumina; all at pH 7and IS of 0.01 M.

the adsorption rate of DCAA onto the adsorbents, the pseudo-first-order equation of Lagergren (1) and the pseudo-second-order rate (2) were evaluated based on the experimental data and the respective kinetic constants of each adsorbent were calculated and listed in Table 2.

A pseudo-second-order model best fitted the adsorption of DCAA onto every tested adsorbent, indicated by the correlation coefficients, compared with the pseudo-first-order model. Thus a pseudo-second-order rate model can be used to describe the adsorption kinetics for DCAA adsorption, based on the assumption

**Table 2**
Kinetics values calculated for DCAA adsorption onto PAC, HMS, A-HMS, M-HMS, activated alumina, NaY and HY zeolite.

| Adsorbent | Pseudo-first-order | | Pseudo-second-order | | | | |
|---|---|---|---|---|---|---|---|
| | $R^2$ | $k_1$ ($h^{-1}$) | $R^2$ | $k_2$ (g/µg h) | Calculated $q_e$ (µg/g) | Experimental $q_e$ (µg/g) | $h^*$ (µg/g h) |
| PAC | 0.721 | 1.997 | 1.000 | 0.094 | 38.760 | 38.605 | 141.220 |
| HMS | 0.723 | 0.159 | 0.986 | 0.073 | 12.438 | 12.141 | 11.293 |
| A-HMS | 0.874 | 1.649 | 1.000 | 0.523 | 5.924 | 5.801 | 18.354 |
| M-HMS | 0.982 | 0.596 | 0.996 | 0.210 | 8.418 | 7.692 | 14.881 |
| NaY | 0.941 | 0.286 | 0.994 | 0.154 | 10.406 | 10.179 | 16.676 |
| HY | 0.931 | 0.313 | 0.997 | 0.254 | 11.655 | 11.290 | 34.503 |
| Alumina | 0.612 | 0.115 | 0.994 | 0.152 | 10.299 | 10.095 | 16.123 |

* $h$ = initial adsorption rate (µg/g h) calculated from $h = k_2 q_e^2$.

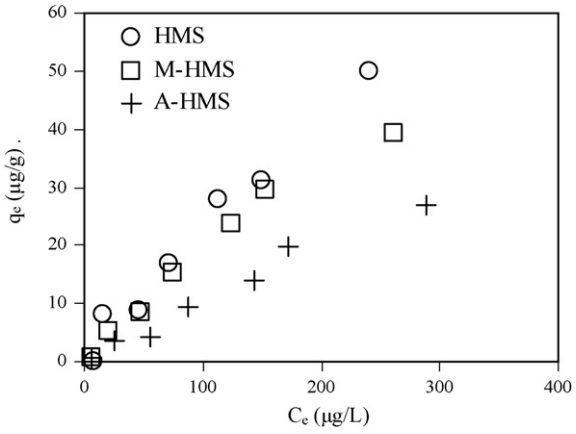


**Fig. 6.** Adsorption capacities of HMS, M-HMS and A-HMS; pH 7, IS 0.01 M.

that the adsorption step may involve chemisorption. Moreover, as shown in Table 2, the comparison of the experimental $q_e$ values and the calculated $q_e$ obtained from the linear plot in Eq. (2) exhibited a very good consistency for all adsorbents

### 3.4. Adsorption isotherm

The adsorption capacity of HMS was plotted against other adsorbents, as $q_e$ versus $C_e$. Comparative plots between HMS and M-HMS and A-HMS were to compare the effects of surface functional groups on DCAA adsorption capacities (Fig. 6), whilst those against NaY

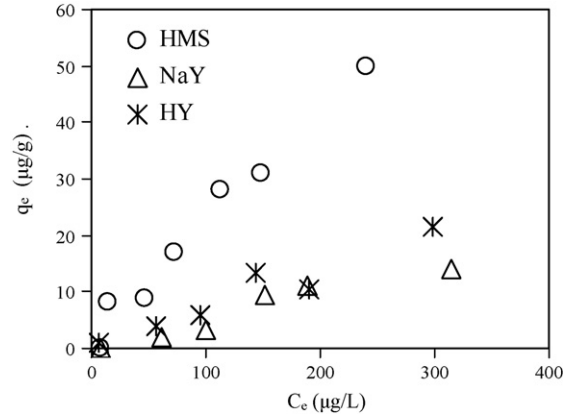


**Fig. 7.** Adsorption capacities of HMS, NaY and HY zeolite; pH 7, IS 0.01 M.

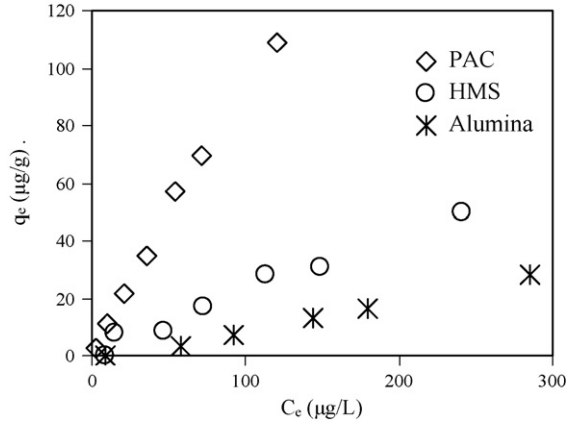


**Fig. 8.** Adsorption capacities of PAC, HMS and activated alumina; pH 7, IS 0.01 M.

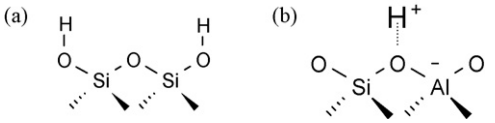


**Fig. 9.** Schematic surface structure and functional groups of (a) HMS (silanol groups) and (b) HY zeolite (Brönsted acid sites).

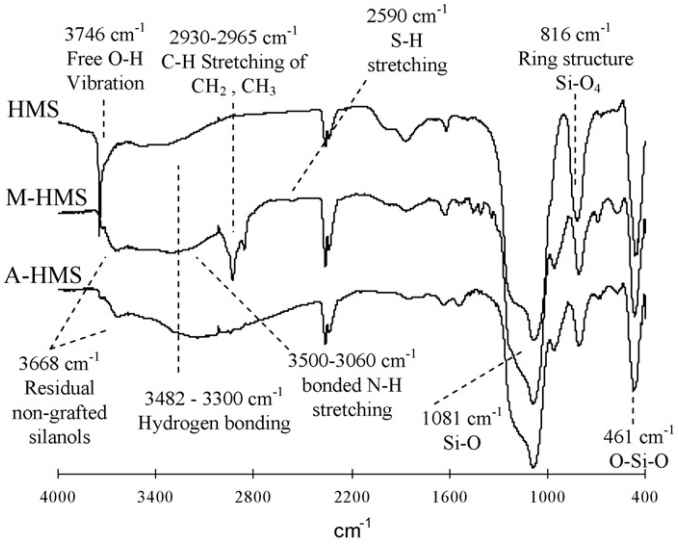


**Fig. 10.** Representative FT-IR spectra of HMS, A-HMS and M-HMS.

**Table 3**
Parameters of Langmuir and Freundlich isotherm model for DCAA adsorption on PAC, HMS, the two functionalized HMS, activated alumina, NaY and HY zeolite at pH 5, 7 and 9.

| Adsorbents | Langmuir | | Freundlich | | | |
|---|---|---|---|---|---|---|
| pH | $q_m$ | $K_L$ | $R^2$ | $K_F$ | $n$ | $R^2$ |
| PAC | | | | | | |
| 5 | 322.581 | 0.0086 | 0.987 | 1.102 | 0.820 | 0.980 |
| 7 | 294.118 | 0.0040 | 0.996 | 0.991 | 1.000 | 0.994 |
| 9 | 7.788 | 0.0415 | 0.935 | 0.928 | 2.587 | 0.865 |
| HMS | | | | | | |
| 5 | 250.000 | 0.0006 | 0.994 | 0.157 | 1.055 | 0.987 |
| 7 | 256.410 | 0.0010 | 0.986 | 0.904 | 1.420 | 0.886 |
| 9 | 212.766 | 0.0003 | 0.987 | 0.024 | 0.820 | 0.950 |
| A-HMS | | | | | | |
| 5 | 322.581 | 0.0004 | 0.991 | 0.158 | 1.104 | 0.983 |
| 7 | 312.500 | 0.0003 | 0.980 | 0.091 | 0.980 | 0.976 |
| 9 | 285.714 | 0.0001 | 0.993 | 0.024 | 0.878 | 0.922 |
| M-HMS | | | | | | |
| 5 | 243.902 | 0.0013 | 0.997 | 0.397 | 1.152 | 0.988 |
| 7 | 238.095 | 0.0011 | 0.994 | 0.175 | 0.949 | 0.994 |
| 9 | 185.185 | 0.0001 | 0.984 | 0.004 | 0.652 | 0.976 |
| NaY | | | | | | |
| 5 | 17.123 | 0.0008 | 0.981 | 0.004 | 0.638 | 0.993 |
| 7 | 26.110 | 0.0038 | 0.983 | 0.001 | 0.585 | 0.980 |
| 9 | 16.863 | 0.0002 | 0.984 | 0.0003 | 0.491 | 0.995 |
| HY | | | | | | |
| 5 | 23.753 | 0.0210 | 0.994 | 0.636 | 1.338 | 0.999 |
| 7 | 15.674 | 0.0086 | 0.991 | 0.159 | 1.200 | 0.966 |
| 9 | 13.459 | 0.0003 | 0.978 | 0.0003 | 0.497 | 0.999 |
| Alumina | | | | | | |
| 5 | 24.155 | 0.0483 | 0.983 | 1.435 | 1.691 | 0.975 |
| 7 | 16.667 | 0.0006 | 0.969 | 0.003 | 0.602 | 0.990 |
| 9 | 15.314 | 0.0027 | 0.693 | 0.002 | 0.613 | 0.963 |

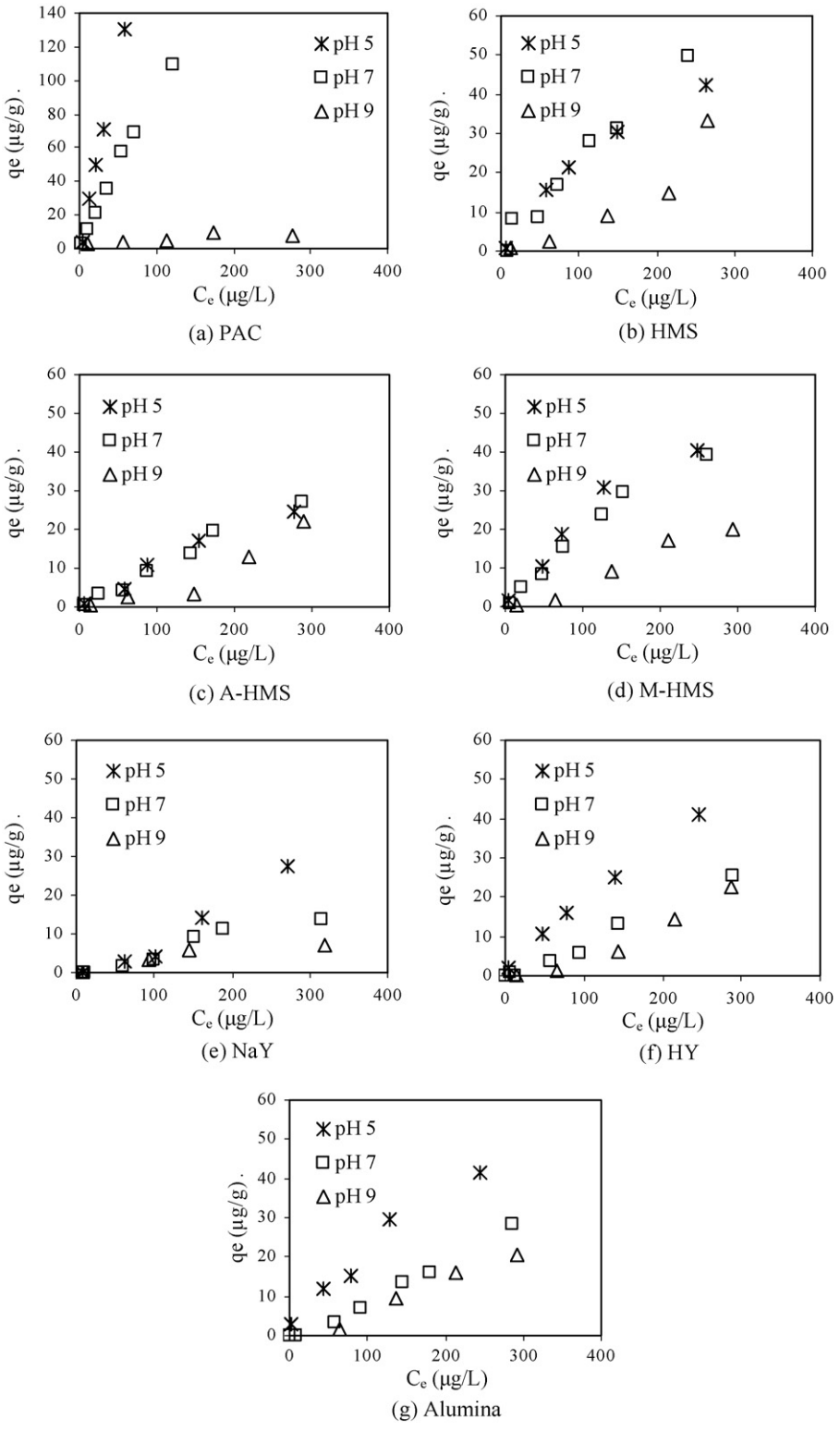


**Fig. 11.** Adsorption capacities of (a) PAC, (b) HMS, (c) A-HMS, (d) M-HMS, (e) NaY, (f) HY and (g) activated alumina, at a pH of 5, 7 or 9; and IS of 0.01 M.

and HY were to compare the effects of micro and mesoporous crystalline structures (Fig. 7), and finally against PAC and alumina (Fig. 8) for general structural comparisons. HMS and M-HMS had similar but higher DCAA adsorption capacities than A-HMS. However, after comparing the adsorption capacities per unit surface area (0.11, 0.7 and 0.04 mg/m$^2$ for A-HMS, HMS and M-HMS respectively), it can be suggested that the combination of hydrogen bonding and attractive electrostatic force (at pH 7) of the amino functional groups enhanced the adsorption capacities per unit surface area.

Pristine HMS also had a significantly higher DCAA adsorption capacity than NaY and HY zeolites both of which have relatively low surface area and small amount of silanol groups [17], being considered as the major functional group for the DCAA adsorption over HMS. An isomorphous substitution of aluminum for tetrahedral sil-

icon in the zeolite framework results in the formation of bridging hydroxyl group, so-called Brönsted acid site (Fig. 9(b)). The positive charge of hydrogen of this site suggested that the DCAA adsorption occurred via an electrostatic force, which can be interfered by the presence of large amount of water, especially in our case with the low concentration of DCAA. Moreover, the microporous structures of zeolite may hamper the accessibility of hydrated DCAA molecules to the adsorption sites.

PAC showed a much higher adsorption capacity than HMS and activated alumina, which might be caused by the surface complexity of PAC inducing many interaction forces, such as electrostatic and van der Waals forces and covalent bonding. Activated alumina showed the lowest DCAA adsorption capacity than HMS, consistence with its lowest surface area compare to each other. Thus, it is clear that the crystalline structure of the adsorbent can significantly affect the adsorption capacity of DCAA.

Adsorption mechanisms due to hydrogen bonding, which is one of the dipole–dipole interactions, can be interfered with by water, especially at a low concentration. Thus, at low concentrations of DCAA (or high concentrations of water) any polar surface can undergo hydrogen bonding with water rather than attract the polar DCAA molecule dissolved in water. Therefore, removal of polar DCAA with ionic functional groups at a low concentration can be affected by water. This fact makes the adsorption capacities of A-HMS lower than the respective ones of PAC. This result is different from that at high DCAA concentrations [9,18]. It was expected that A-HMS, which exhibits a positive charge on its surface, could enhance the adsorption capacity for DCAA by electrostatic attraction with the negative charge of DCAA. However, it was found that at low concentrations the electrostatic attraction did not seem to increase significantly the adsorption capacity of A-HMS. Another possible reason for the lower than expected adsorption capacity of A-HMS could be the low surface area of A-HMS, due to the collapse of the crystalline structure caused by the pre-grafting method.

Unexpectedly, M-HMS, which has a higher hydrophobicity and an almost neutral charge, exhibited a comparable adsorption capacity to that for HMS. Perhaps, the higher surface area as well as residual silanol groups (non-grafted silanol) remaining on surface of M-HMS, as supported by the FT-IR spectra (Fig. 10) can affect the adsorption of DCAA at low concentrations. In Fig. 9, the FT-IR spectra gives evidence of Si–O–Si bonds by the adsorption peaks at around 470, 800 and 1070 $cm^{-1}$. Furthermore, the presence of organic functional groups was also supported by the peaks at 2930–2965 $cm^{-1}$ which likely corresponded to CH stretching. The sharp peak at 3746 $cm^{-1}$ of pristine HMS is due to the OH-stretching of non-hydrogen-bonded Si–OH. Stretching of the residual non-grafted Si–OH in both M-HMS and A-HMS had a peak at 3668 $cm^{-1}$.

The parameters and correlation coefficients of the Langmuir and Fruendlich isotherm models, calculated by using experimental data through linear regression, are listed in Table 3. The correlation coefficients of Langmuir and Freundlich isotherms were not different significantly (except for PAC at pH 9, HMS at pH 7 and especially alumina at pH 9 which is drastically different as presented in the table). The data were also plotted by non-linear estimation of STATISTICA version 6.0 which revealed no strong relationship with the Langmuir isotherm, but in contrast the Freundlich isotherm fitted the data with very high correlation coefficients.

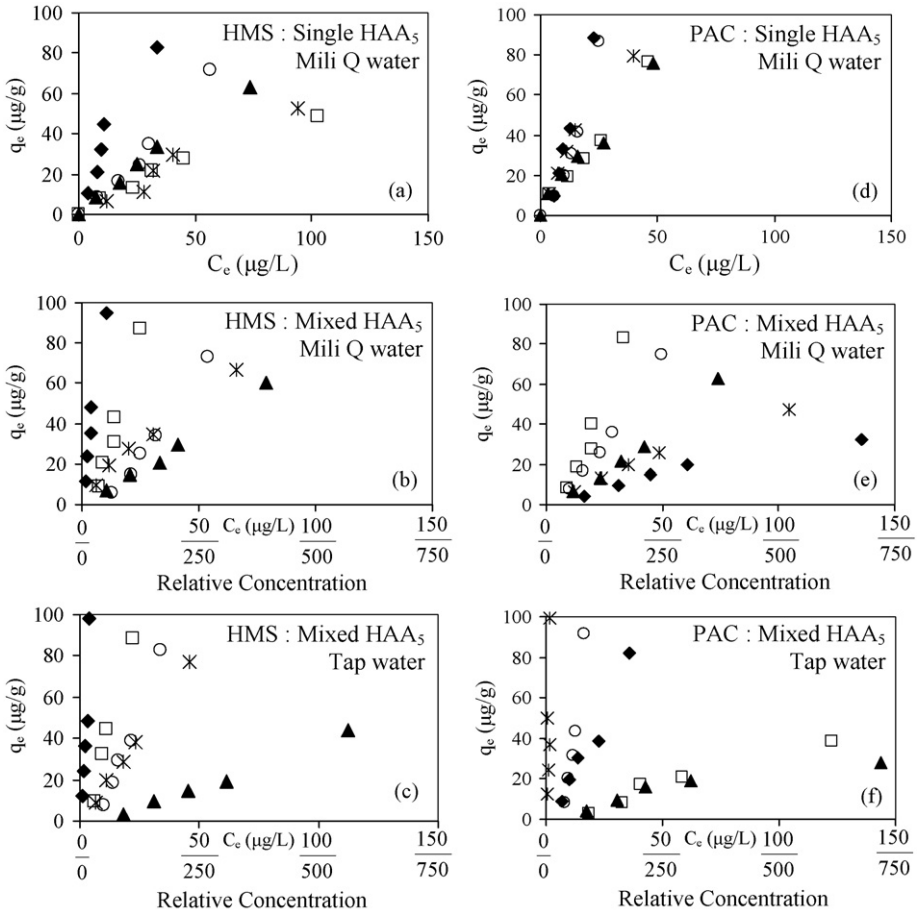


**Fig. 12.** PAC and HMS Adsorption isotherms of $HAA_5$ groups in single-solute and mixed-solute (milli-Q water) at pH 7, 25 °C and IS 0.01 M, comparing with adsorption isotherms of mixed solute $HAA_5$ groups in tap water (♦: MCAA, □: DCAA, ▲: TCAA, ○: MBAA, ×: DBAA).

An increase of temperature from 25 to 60 °C did not effect to DCAA adsorption capacity of pristine HMS significantly. However, DCAA adsorption capacity of PAC slightly decreased with increasing temperature (data not shown).

### 3.5. Effect of pH

The electrostatic interaction between ionic species and ionic surface functional groups is known to be highly dependent on pH. The adsorption capacities of all adsorbents within a pH range from 5 to 9 was evaluated and is summarized in Fig. 11, where the adsorption capacity of all adsorbents at pH 9 was lower than that at pH 7 and 5, presumably because of the repulsion force between the negative charge of the adsorbent surface and that of DCAA. Moreover, at a pH higher than the respective pHzpc the surface functional groups can be ionized, as discussed in Section 3.2, and that can strongly affect the hydrogen bonding between DCAA and surfaces.

The surfaces of PAC, activated alumina, HY and NaY zeolite at pH 5 have a higher positive charge leading to a higher adsorption capacity than that at pH 7 or 9. DCAA adsorption was significantly affected by the pH, but the adsorption capacities of A-HMS and M-HMS were not significantly affected by increasing the pH from 5 to 7, since the effect of the positive surface charge at pH 5 and 7 did not change significantly due to very high $pH_{zpc}$ at 9.5 of A-HMS, and the lower effect of hydrogen bonding of mercapto-functional groups of M-HMS, compared to the silanol and amino groups. In addition, no effect of pH on the adsorption capacities of pristine HMS was evident from pH 5 to 7, being observed only when the pH was increased up to 9, since the neutral charge of the HMS surface does not change significantly within pH 4–6.

### 3.6. Selective adsorption of $HAA_5$ groups and effect of electrolytes in tap water

Fig. 12(a) and (d) shows the results of batch adsorption in single-solute solution of each $HAA_5$ on HMS and PAC, respectively. MCAA which had lowest molecular weight exhibited the highest adsorption capacities on both HMS and PAC. However, adsorption capacities of $HAA_5$ on HMS did not clearly relate to the type and amount of halogen atom in the molecule, but for PAC monohaloacetic acids (MCAA and DBAA) had slightly higher adsorption capacities, compared with di and tri-haloacetic acids. Moreover, the results of competitive adsorption of multiple-solute on HMS and PAC surfaces are shown in Fig. 12(b) and (e). It was found that order of adsorption capacities of $HAA_5$ on HMS and PAC was totally different from single-solute solution results. It can be seen that adsorption capacities of HMS for $HAA_5$ clearly related to $pK_a$ value and halogen atom of $HAA_5$, such as MCAA > DCAA > TCAA for chloroacetic acid and MBAA > DBAA for bromoacetic acid. Low $pK_a$ $HAA_5$ (TCAA and DBAA) are supposed high potential to interact with hydronium ion in the water, which can reduce charge density of molecule and accessibility to active site of HMS surface. However, effect of surface interaction between complex surface functional groups of PAC and $HAA_5$ on capacities and selective adsorption is still unclear. Common electrolytes in tap water such as $Na^+$, $Mg^{2+}$, $Ca^{2+}$, $Cl^-$, $F^-$, $NO_3^-$, $SO_3^{2-}$ and $HCO_3^-$, measured by ion chromatography (19.2, 5.2, 19.3, 21.13, 0.32, 0.79, 22.8 and 20.0 mg/L, respectively.), did not affect the adsorption capacities and selectivity of HMS for $HAA_5$ in the multiple-solute solution, significantly (Fig. 12(c) and (f)). However, a slightly increase of the adsorption capacities and selectivity of PAC for DBAA, MBAA and MCAA was detected.

## 4. Conclusions

The adsorption kinetics for DCAA adsorption on all adsorbents followed the pseudo-second-order model. DCAA adsorption capacity at a low concentration is strongly affected by physical characteristics (e.g. surface area and silicate structure) caused by their own crystalline structure. The interaction between DCAA and adsorbents involves hydrogen bonding and electrostatic forces related to $pH_{zpc}$ of adsorbents, caused by surface functional groups. Decreasing the pH to less than the $pH_{zpc}$ can increase the DCAA adsorption capacity. Adsorption of $HAA_5$ on HMS did not relate to molecular structure of $HAA_5$. Unlike PAC, common electrolytes did not affect to $HAA_5$ adsorption capacity and selectivity of HMS.

## Acknowledgements

The authors express gratitude to the Thailand Research Fund, Thailand under grant no. MRG5080177 and the 90th Anniversary of Chulalongkorn University Fund (Ratchadphiseksomphot Endowment Fund) for financial support. The support by Center of Excellence for Petroleum, Petrochemicals and Advanced Materials is also acknowledged.

## References

[1] K.G. Lee, B.H. Kim, J.E. Hong, H.S. Pyo, S.J. Park, D.W. Lee, A Study on the distribution of chlorination by-products (CBPs) in treated water in Korea, Water Res. 35 (2001) 2861–2872.
[2] D. Martinez, F. Borrull, M. Calull, Comparative study of solid-phase extraction system coupled to capillary electrophoresis in the determination of haloacetic compounds in tap water, J. Chromatogr. A 827 (1998) 105–112.
[3] M.N. Sarrión, F.J. Santos, M.T. Galceran, In situ derivatization/solid-phase microextraction for the determination of haloacetic acids in water, Anal. Chem. 72 (2000) 4865–4873.
[4] T.K. Nissinen, I.T. Miettiene, P.J. Martikainen, T. Vartiainen, Disinfection by-products in Finnish drinking water, Chemosphere 48 (2002) 9–20.
[5] US Environmental Protection Agency, Controlling Disinfection By-products and Microbial Contaminants in Drinking Water, Washington, D.C., Office of Research and Development, 2001.
[6] G.V. Korshin, M.D. Jenson, Electrochemical reduction of haloacetic acids and exploration their removal by electrochemical treatment, Electrochim. Acta 47 (2001) 747–751.
[7] H.H. Tung, R.F. Unz, Y.F. Xie, HAA removal by GAC adsorption, J. Am. Water Works Assoc. 98 (6) (2006) 107–112.
[8] Y.F.F. Xie, H.J. Zhou, Use of BAC for HAA removal-Part 2, column study, J. Am. Water Works Assoc. 94 (5) (2002) 126–134.
[9] P. Punyapalakul, S. Takizawa, Effect of organic grafting modification of hexagonal mesoporous silicate on haloacetic acid removal, Environ. Eng. Forum 44 (2004) 247–256.
[10] P.T. Tanev, T.J. Pinnavaia, Mesoporous silica molecular sieves prepared by ionic and neutral surfactant templating: a comparison of physical properties, Chem. Mater. 8 (1996) 2068–2079.
[11] B.H. Lee, Y.H. Kim, H.J. Lee, J.H. Yi, Synthesis of functionalized porous silicas via templating method as heavy metal ion adsorbents: the introduction of surface hydrophilicity onto the surface of adsorbents, Microporous Mesoporous Mater. 50 (1) (2001) 77–90.
[12] P. Punyapalakul, S. Takizawa, Selective adsorption of nonionic surfactant on hexagonal mesoporous silicate (HMSs) in the present of ionic dyes, Water Res. 40 (2006) 3177–3184.
[13] A.S.M. Chong, X.S. Zhao, A.T. Kustedjo, S.Z. Qiao, Functionalization of large-pore mesoporous silicas with organosilanes by direct synthesis, Microporous Mesoporous Mater. 72 (2004) 33–42.
[14] M.M.J. Treacy, J.B. Higgins (Eds.), Collection of Simulated XRD Powder Patterns for Zeolites, 4th edition, Elsevier, 2001, pp. 150–151.
[15] S. Gontier, A. Tuel, Synthesis and charaterization of Ti-containing mesoporous silicas, Zeolites 15 (1995) 601–610.
[16] Q. Yu, S. Deng, G. Yu, Selective removal of perfluorooctane sulfonate from awueous solution using chitosan-based molecularly imprinted polymer adsorbents, Water Res. 42 (2008) 3089–3097.
[17] W.W. John, The nature of active sites on zeolites, II temperature dependence of the infrared spectra of hydrogen Y zeolite, J. Catal. 9 (1967) 396–402.
[18] J.C. Crittenden, R.R. Trussell, D.W. Hand, K.J. Howe, G. Tchobanoglous, Water Treatment: Principles and Design, 2nd ed., John Wiley & Sons, Inc., Hoboken, NJ, 2005.